Radiative decay of the 4d⁵(⁶S)5p z^{5,7}Pᵒ states in Tc II: comparison along the homologous and isoelectronic sequences. Application to astrophysics

P. Palmeri,[1] P. Quinet,[1,2] É. Biémont,[1,2]★ A. V. Yushchenko,[3,4] A. Jorissen[5]
and S. Van Eck[5]

[1]*Astrophysique et Spectroscopie, Université de Mons-Hainaut, 7000 Mons, Belgium*
[2]*IPNAS, Bât. B15, Université de Liège, Sart Tilman 4000 Liège, Belgium*
[3]*Astronomical Observatory, Odessa National University, Parc Shevchenko, Odessa 65014, Ukraine*
[4]*Astronomical Research Center for the Structure and Evolution of the Cosmos, Sejong University, Seoul, 143-747, South Korea*
[5]*Institut d' Astrophysique, Université Libre de Bruxelles, 1050 Bruxelles, Belgium*

ABSTRACT

Using three independent theoretical approaches (CA, HFR + CP, AUTOSTRUCTURE), oscillator strengths have been calculated for a set of Tc II transitions of astrophysical interest and the reliability of their absolute scale has been assessed. The examination of the spectra emitted by some Ap stars has allowed the identification of Tc II transitions in HD 125248. This Tc II detection should however await confirmation from spectral synthesis relying on dedicated model atmospheres. New partition functions are also provided for Tc I, Tc II and Tc III for temperatures ranging between 4000 and 13 000 K.

Key words: atomic data – atomic processes – line: identification – stars: AGB and post-AGB – stars: chemically peculiar.

1 THE ASTROPHYSICAL CONTEXT

In astrophysics, technetium is an s-process element with no stable isotope. It was first identified in the spectra of some M and S stars by Merrill (1952a,b). The S stars, which appear as a temperature sequence parallel to the M stars, sometimes exhibit technetium in their spectrum and, in that case, they are called intrinsic S stars. When Tc lines are lacking, these stars are referred to as extrinsic S stars (Iben & Renzini 1983; Little et al. 1987; Smith & Lambert 1988; Busso et al. 1992).

The s-process overabundances in S stars are explained by considering the thermally pulsing asymptotic giant branch (TPAGB) evolution. The He- and C-rich layer residing below the H-burning shell in AGB stars provides an adequate environment for the s-process nucleosynthesis, which only produces the isotope 99 of Tc (laboratory half-life of 2.1×10^5 yr, falling to about 40 yr at the high temperatures $T > 2 \times 10^8$ K met in the intershell region of high-mass AGB stars; Coster & Truran 1981; Schatz 1983). The s-process operates when protons from the overlying H-rich shell are mixed into the He- and C-rich shell just following a thermal pulse (Straniero et al. 1995; Goriely & Mowlavi 2000). S-process elements may then be brought to the surface of the star by the so-called third dredge-up. Technetium should thus be detectable during about 1.0×10^6 yr (Smith & Lambert 1988) and, if the dredge-up process occurs after each thermal pulse, Tc should be observed in all TPAGB stars. Some S stars do not show Tc lines in their spec-

trum (see e.g. Little-Marenin & Little 1979; Little, Little-Marenin & Hagen-Bauer 1987). It is generally believed that these technetium-poor stars are resulting from a totally different evolutionary scheme: the accretion long ago of s-process-rich matter from a companion, in a binary system, explains their chemical peculiarities and the absence of Tc (see e.g. Smith & Lambert 1987, 1988; Jorissen & Mayor 1988, 1992; Brown et al. 1990; Johnson, Ake & Ameen 1993; Jorissen et al. 1993).

Extrinsic and intrinsic S stars can also be distinguished using photometric or binarity criteria, but technetium detection remains the safest way to disentangle them (see e.g. Smith & Lambert 1990; Busso et al. 1992). In a recent analysis, the Tc/no Tc dichotomy was considered by Van Eck & Jorissen (1999, 2000) in the Henize sample of S stars. Among the 70 analysed objects, 41 turned out to be technetium-poor and 29 technetium-rich on the basis of the analysis of the two Tc I lines at 423.8 and 426.2 nm.

To detect Tc I in the S stars, high-resolution spectra are needed because resonance transitions appear in the ultraviolet (UV) region where blending problems are present. In red giants, the Tc transitions are frequently saturated and also affected by hyperfine-structure effects. In addition, until recently (see Palmeri & Wyart 1989; Palmeri et al. 2005a), transition probabilities were missing. Consequently, the quantitative analysis of these stellar spectra is not easy.

In hotter stars ($T_{\rm eff} > 4000$ K), the dominant ion is Tc II according to Saha equation but the most intense lines appear in the UV region (264.70, 261.00 and 254.32 nm), a spectral range accessible only from space. In fact, up to now, little has been done concerning the analysis of Tc II lines in stellar spectra. The search for the lines at 264.702, 261.000 and 254.324 nm in *International Ultraviolet*

★E-mail: E.Biemont@ulg.ac.be

Explorer (*IUE*) spectra of the barium stars HR 5058, o Vir and ζ Cap was not successful (Little-Marenin & Little 1987), the lack of Tc II implying that the observed s-process enhancements were produced more than half a million years ago. Davis (1973) suggested that Tc II lines might be present in the spectra of some Ap stars. Boyarchuk & Snow (1978), using UV spectra from the *Copernicus* satellite, could detect Tc II lines neither in the Am star Sirius nor in the A0V star Vega. These analyses however suffer from the lack of atomic data for Tc II. The main aim of this paper is to fill in this gap and to provide a reliable set of transition probabilities for Tc II transitions of astrophysical interest.

2 THE ATOMIC CONTEXT

Technetium ($Z = 43$) has three long-lived ($\tau \geqslant 2.1\,10^5$ yr) ^{97}Tc, ^{98}Tc, ^{99}Tc and 20 short-lived isotopes and isomers, ^{99}Tc being the isotope produced by the s-process.

The ground state configuration of singly ionized technetium (Tc II) is 4d^{5}5s a^{7}S$_3$ (Moore 1958) and the ionization energy is 123 100 cm^{-1} (15.26 eV), a value deduced by Catalan & Rico (1952). All technetium isotopes are radioactive and this radioactivity is responsible of the scarcity of spectroscopic experimental investigations. In addition, the complexity of the electronic structure of the 4d elements has prevented so far the use of theoretical approaches for investigating the radiative parameters of Tc II.

The Tc II spectrum was first observed by Meggers & Scribner (1950) and an analysis was reported by Meggers (1951). The levels quoted by Moore (1958) (33 levels) originate essentially from unpublished observations by Meggers & Catalan (unpublished) and Bozman (unpublished). Some levels however are affected by unknown uncertainties due to the fact that observations short of 205.4 nm are not available. The level values adopted in the more recent NIST compilation are taken directly from Moore (1958). The persistent lines of Tc II originate from more recent observations due to Bozman, Meggers & Corliss (1967). These authors have provided a new and more complete description of Tc I and Tc II spectra in the region 200.0–900.0 nm where about 4500 transitions were produced with arc and spark sources. 1200 of these transitions were due to Tc II.

Transition probabilities in Tc II are very scarce. While some recent works have provided a number of results in neutral technetium (Palmeri & Wyart 1999; O'Malley & Beck 2003; Palmeri et al. 2005a), no similar attempts exist for singly ionized technetium. To our knowledge, the only transition probabilities available in Tc II are due to Bakhtiyarov (1988). These results however were obtained through single-configuration calculations and the length-form data differed substantially (up to 40 per cent) from the velocity-form results.

In the present paper, thanks to the combined use of three independent theoretical approaches, we provide a reliable set of transition probabilities for Tc II transitions originating from the z^{5}P$^o_{1,2,3}$ and z^{7}P$^o_{2,3,4}$ levels. This set of results is then used for a search for Tc II lines in several stellar spectra.

3 COMPUTATIONAL STRATEGY

The lack of experimental and theoretical radiative rates in Tc II has led us to consider three different independent semi-empirical or theoretical approaches, namely the pseudo-relativistic Hartree–Fock method of Cowan (1981) with a core-polarization (CP) model potential (HFR + CP), the Coulomb approximation (CA) of Bates &

Damgaard (1949) and a multiconfigurational Breit-Pauli approximation using a scaled Thomas–Fermi potential implemented in the AUTOSTRUCTURE code (Badnell 1986, 1997). Moreover, assessment of the methods used was done by comparing calculations made in similar conditions along the homologous and isoelectronic sequences for ions for which reliable lifetime measurements obtained by laser-induced fluorescence (LIF) techniques were available, that is, Mn II (Pinnington et al. 1992), Re II (Palmeri et al. 2005b) and Mo I (Kwiatkowski et al. 1981; Schnehage et al. 1983).

3.1 The Coulomb approximation calculations

The CA approximation of Bates & Damgaard (1949) is a well-established monoconfiguration approach which has been extensively used in the past (see e.g. Biémont & Grevesse 1973; Lindgard & Nielsen 1977). This method does generally provide accurate transition probabilities when configuration interaction (CI) is very weak and when transitions involving only an optical (thus non-penetrating) electron are concerned. This is the case, for example, for many transitions in alkali-like ions.

For complex systems, the simple CA appears to meet with considerable success although it is not easy to lay down comprehensive rules to delineate the range of applicability. Nevertheless, the method is expected to provide accurate to fair results for the transitions for which the levels involved belong to two categories: first, the levels for which the active electron is in a shell by itself and for which the exchange forces are relatively small (thus the moderately and highly excited levels); secondly, the levels for which the active electron is in a shell containing other electrons or for which the exchange forces are relatively large as is the case for the ground and usually the lower excited levels. The conditions of applicability of the method are thus expected to be met for the a^{7}S–z^{7}P^o and for the a^{5}S–z^{5}P^o transitions in Tc II.

In Re II, strong CI is expected to affect the spectrum as indicated by the experimental lifetime values obtained for this ion. It appears indeed that the lifetime value for $J = 1$ in the ^{5}P^o term is larger by more than a factor of 4 than the time-resolved LIF measurements (Palmeri et al. 2005b) for the other J values within the same multiplet. CA is therefore not expected to provide reliable results in this ion and, consequently, is not applied to Re II.

In Mo I, the transitions originating from the ^{5}P$^o_{1,2,3}$ levels are falling within the range of applicability of the CA while this is no more the case for the transitions originating from z^{7}P$^o_{2,3,4}$ according to the tables in the original paper of Bates & Damgaard (1949). These tables were used in fact for the calculations in combination with the generalized tables of line strengths given by White & Eliason (1933) and Shore & Menzel (1965). The CA results are reported in Tables 1 (lifetime values) and 2 (oscillator strengths).

3.2 The HFR + CP approach

The pseudo-relativistic Hartree–Fock (HFR) option of the RCN code (Cowan 1981) was used to get the atomic orbitals of Tc II and the following configurations were retained in the CI expansion: nd^5n''s + nd^4n'sn''s + nd^6 + nd^5n'd + nd^4n'sn'd + nd^3n's^2n'd + nd^4n'p^2 for the even parity; nd^5n''p + nd^4n'sn''p + nd^3n's^2n'p for the odd parity, where $n = 3$ in Mn II, $n = 4$ in Mo I and Tc II, $n = 5$ in Re II, $n' = n + 1$, and $n'' = (n + 1)$, $(n + 2)$ and $(n + 3)$. It represented a total of 3870 energy levels in each atomic system. The inclusion of more configurations was prevented by the computer limits. The Slater integrals were scaled down by 0.80 (see Cowan 1981, for a justification).

Besides these intravalence correlations, core–valence interactions can be taken into account using a CP model potential and a correction to the electric dipole transition operator, both depending on two parameters (the dipole polarizability of the ionic core, α_d, and the cut-off radius, r_c). This technique has been implemented in Cowan's codes and described in details elsewhere (Biémont et al. 2000). The complexity of configurations with open d subshells and the experience gained in similar treatments in Tc I (Palmeri et al. 2005a) and in Lu I (Fedchak et al. 2000) have suggested to us to attempt two different CP models: CP1 and CP2.

In the first one (CP1), we considered a $1s^2 \cdots np^6$ core surrounded by 6 valence electrons. In Tc II ($n = 4$), the adopted CP parameters were $1.439\,a_0^3$ for the polarizability (Johnson, Kolb & Huang 1983) and $1.19\,a_0$ for the cut-off radius, that is, the *ab initio* HFR average value $\langle r \rangle$ for the outermost core orbital, 4p. Concerning the other ions, the parameter values were: $\alpha_d = 0.6271\,a_0^3$ (Johnson et al. 1983) and $r_c = \langle 3p|r|3p \rangle_{HFR} = 0.92\,a_0$ for Mn II ($n = 3$); $\alpha_d = 1.789\,a_0^3$ (Johnson et al. 1983) and $r_c = \langle 4p|r|4p \rangle_{HFR} = 1.25\,a_0$ for Mo I ($n = 4$); $\alpha_d = 2.58\,a_0^3$ and $r_c = \langle 5p|r|5p \rangle_{HFR} = 1.22\,a_0$ for Re II ($n = 5$). In the case of Re II, no polarizability value was available in the literature for the Re VIII ionic core. It was therefore determined by extrapolation from the Fraga, Karwowski & Saxena (1976) values along the Er isoelectronic sequence as illustrated in Fig. 1.

In the second model (CP2), different ionic cores were used for the different types of configurations corresponding to different occupation numbers of the nd subshell (nd^6, nd^5, nd^4 and nd^3). For the configurations nd^6, the same CP parameters as in CP1 were chosen. For the other configurations, we considered A^{2+}, A^{3+} and A^{4+} ionic cores, depending on the number of electrons in the nd subshell, that is, five, four or three electrons, respectively, where A = Mn, Tc, Re. In the case of Mo I and Mo$^+$, Mo^{2+} and Mo^{3+} cores were used, respectively. This choice corresponds to the following dipole polarizabilities (Fraga et al. 1976): 3.10, 1.82, 1.21 a_0^3 for Mn II; 17.54, 9.38, 5.67 a_0^3 for Mo I; 8.43, 5.40, 3.64 a_0^3 for Tc II; 10.39, 6.81, 4.72 a_0^3 for Re II. The HFR average value $\langle r \rangle$ for the nd orbitals calculated in each configuration were chosen as the cut-off radii in the CP model potential. As different core parameters were considered for the initial and the final configurations of each transition array, the algebraic mean of the α_d values and the geometric mean of the r_c values deduced, respectively, for the initial and the final configurations of a transition were used in the correction of the E1 transition operator.

The energy parameters were fitted in order to minimize the differences between the eigenvalues and the available experimental energy levels by means of the least-squares fitting program RCE (Cowan 1981). In Tc II, the 13 reliable energy levels, that is, the ground term $4d^5(^6S)5s\ a^7S$ and the first excited even terms $4d^5(^6S)5s\ a^5S$, $4d^6\ a^5D$ and odd terms $4d^5(^6S)5p\ z^{7,5}P^o$, compiled by Moore (1958), were used to fit nine radial parameters, namely the average energies of the configurations $4d^55s$, $4d^6$, $4d^55p$, $G^2(4d,5s)$ of $4d^55s$, ζ_{4d} of $4d^6$ and ζ_{4d}, ζ_{5p}, $G^{1,3}(4d,5p)$ of $4d^55p$. The *ab initio* $G^1(4d,5p)/G^3(4d,5p)$ ratio was kept constant. The s.d. values were 9 and 25 cm^{-1} for the even and odd parities, respectively. Focusing on the assessment of the method used in Tc II, similar number and types of experimental energy levels have been considered in the least-squares fits for the other ions, that is, $3d^5(^6S)4s\ a^{7,5}S$, $3d^6\ a^5D$ and $3d^5(^6S)4p\ z^{7,5}P^o$ in Mn II compiled by Sugar & Corliss (1985), $5d^5(^6S)6s\ a^{7,5}S$, $5d^46s^2\ a^5D$ and $5d^5(^6S)6p\ z^{7,5}P^o$ in Re II (Moore 1958; Wahlgren et al. 1997), and $4d^5(^6S)5s\ a^{7,5}S$ and $4d^5(^6S)5p\ z^{7,5}P^o$ in Mo I (Whaling & Brault 1988). In Mn II, the radial integrals E_{av}, $G^2(3d,4s)$ of $3d^54s$, E_{av}, ζ_{3d} of $3d^6$ and E_{av}, ζ_{3d}, ζ_{4p}, $G^{1,3}(3d,4p)$ of $3d^54p$ were fit-

Table 1. Comparison of radiative lifetimes of the $z^{5,7}P^o$ levels in Mn II, Tc II, Re II and Mo I.

| Ion | Level | Lifetime (ns) | | |
		Exp.[a]	HFR + CP1[b]	HFR + CP2[c]	CA[d]
Mn II	$z^7P_2^o$	3.66(5)[e]	3.21	3.98	3.44[e]
	$z^7P_3^o$	3.60(5)[e]	3.17	3.98	3.39[e]
	$z^7P_4^o$	3.54(5)[e]	3.10	3.84	3.32[e]
	$z^5P_1^o$	4.05(10)[e]	3.64	4.35	4.18[e]
	$z^5P_2^o$	4.15(10)[e]	3.64	4.35	4.20[e]
	$z^5P_3^o$	4.24(10)[e]	3.64	4.36	4.24[e]
Tc II	$z^7P_2^o$		3.28	5.06	3.42[f]
	$z^7P_3^o$		3.19	4.91	3.24[f]
	$z^7P_4^o$		2.88	4.44	3.02
	$z^5P_1^o$		3.08	4.28	2.83[f]
	$z^5P_2^o$		3.00	4.18	2.72[f]
	$z^5P_3^o$		2.87	4.00	2.59[f]
Re II	$z^7P_2^o$	4.5(3)	4.16	7.13	See the text
	$z^7P_3^o$	4.6(3)	4.14	7.04	
	$z^7P_4^o$		3.20	5.46	
	$z^5P_1^o$	17.8(1.5)	17.79	26.68	
	$z^5P_2^o$	4.2(3)	5.90	9.23	
	$z^5P_3^o$	3.4(3)	4.55	7.04	
Mo I	$z^7P_2^o$	16.3(8)[g]	16.06	27.53	See the text
	$z^7P_3^o$	15.8(8)[g]	15.02	25.80	
	$z^7P_4^o$	14.7(7)[g]	13.96	24.05	
	$z^5P_1^o$		17.01	26.15	17.34
	$z^5P_2^o$	20.5[h]	17.69	27.27	16.96
	$z^5P_3^o$		18.03	27.76	16.73

[a]Exp.: LIF (Palmeri et al. 2005b). [b] HFR + CP1: HFR calculations with the CP1 core-polarization model (see the text). [c] HFR + CP2: HFR calculations with the CP2 core-polarization model (see the text). [d]CA: Coulomb approximation calculations (this work). [e]Beam-laser measurements and CA calculations by Pinnington et al. (1992). [f]The main channel (most intense transition) has been calculated with the CA (Bates & Damgaard 1949). For the $4d^6$–$4d^55p$ transitions, the HFR values (HFR + CP1) have been considered (see the text). [g]LIF (Kwiatkowski et al. 1981). [h]LIF measurements of Zimmermann et al. reported as a private communication by Schnehage et al. (1983).

ted giving s.d. values of 2 cm^{-1} in both parities. The *ab initio* $G^1(3d,4p)/G^3(3d,4p)$ ratio was also kept constant. In Re II, as the $5d^46s^2\ a^5D_J$ states were strongly mixed within the $(5d+6s)^6$ group, the three average energies and three spin–orbit integrals of this group were varied along with the exchange integral $G^2(5d,6s)$ of $5d^56s$, keeping the HFR ratios of the spin–orbit integrals constant. In the odd parity, the E_{av}, ζ_{5d}, ζ_{6p}, $G^{1,3}(5d,6p)$ radial parameters of $5d^56p$ were fitted fixing the $G^1(5d,6p)/G^3(5d,6p)$ ratio to its HFR value. The s.d. values were 172 and 205 cm^{-1} in the even and odd parities, respectively. In Mo I, the radial parameters E_{av}, $G^2(4d,5s)$ of $4d^55s$, and E_{av}, ζ_{4d}, ζ_{5p}, $G^{1,3}(4d,5p)$ of $4d^55p$ were varied keeping the $G^1(4d,5p)/G^3(4d,5p)$ ratio to its *ab initio* value. The s.d. was 35 cm^{-1} in the odd parity (it was trivially meaningless in the even parity as two parameters fitted two levels). The fitted parameter values are given in Table 3.

The improved eigenvectors resulting from the above least-squares-fitting procedures combined with both CP models (CP1 and CP2) were used for evaluating the radiative lifetimes and oscillator strengths. The results are reported in Tables 1 and 2.

3.3 AUTOSTRUCTURE

AUTOSTRUCTURE, an extension by Badnell (1986, 1997) of the code SUPERSTRUCTURE (Eissner, Jones & Nussbaumer 1974),

Table 2. Comparison of oscillator strengths for transitions depopulating the $4d^5(^6S)5p$ $z^{5,7}P^o$ levels in Tc II.

Transition[a]		λ^b (nm)	log gf^c				
Lower level	Upper level		HFR + CP1	HFR + CP2	AS1	AS2	CA
a^7S_3	$z^7P^o_2$	264.7011	0.20	0.01	0.17	0.19	0.18
a^5S_2	$z^7P^o_2$	397.5017	−1.60	−1.75	−2.00	−1.52	−
a^7S_3	$z^7P^o_3$	260.9995	0.34	0.15	0.32	0.33	0.33
a^5D_4	$z^7P^o_3$	286.9296	−1.65	−1.77	−2.07	−1.44	−
a^5S_2	$z^7P^o_3$	389.2129	−1.14	−1.30	−1.50	−1.05	−
a^7S_3	$z^7P^o_4$	254.3223	0.48	0.29	0.45	0.47	0.46
a^7S_3	$z^5P^o_3$	229.8092	−0.90	−1.09	−1.20	−0.84	−
a^5D_4	$z^5P^o_3$	249.6769	−0.07	−0.20	−0.15	−0.04	−
a^5D_3	$z^5P^o_3$	254.4815	−0.65	−0.78	−0.73	−0.62	−
a^5D_2	$z^5P^o_3$	257.4442	−1.54	−1.67	−1.96	−1.50	−
a^5S_2	$z^5P^o_3$	323.7014	0.24	0.08	0.24	0.24	0.33
a^7S_3	$z^5P^o_2$	228.5462	−1.34	−1.53	−1.62	−1.28	−
a^5D_3	$z^5P^o_2$	252.9338	−0.38	−0.51	−0.46	−0.34	−
a^5D_2	$z^5P^o_2$	255.8603	−0.56	−0.69	−0.33	−0.52	−
a^5D_1	$z^5P^o_2$	257.7864	−1.16	−1.29	−1.24	−1.12	−
a^5S_2	$z^5P^o_2$	321.2013	0.10	−0.05	0.002	0.11	0.19
a^5D_2	$z^5P^o_1$	254.7929	−0.82	−0.95	−1.53	−0.77	−
a^5D_1	$z^5P^o_1$	256.7030	−0.69	−0.82	−0.78	−0.65	−
a^5D_0	$z^5P^o_1$	257.6281	−1.04	−1.17	−1.13	−1.00	−
a^5S_2	$z^5P^o_1$	319.5210	−0.10	−0.26	−0.06	−0.09	−0.03

[a]Designations from Moore (1958). [b]Calculated in air from the experimental energy levels given in Moore (1958). [c]Only the transitions with log $gf > −2$ are tabulated. HFR + CP1: HFR calculations including CP effects considering a seven times ionized core (this work). HFR + CP2: HFR calculations including CP effects considering different ionic cores for the different 4d subshell occupancies (this work). AS1: AUTOSTRUCTURE calculations including CP effects considering a seven times ionized core (this work). AS2: as in AS1 but with TEC. CA: Coulomb approximation calculations (this work). The intercombinations cannot be considered within the framework of the CA and, for the $4d^6$–$4d^5 5p$ transitions, the CA is not applicable.
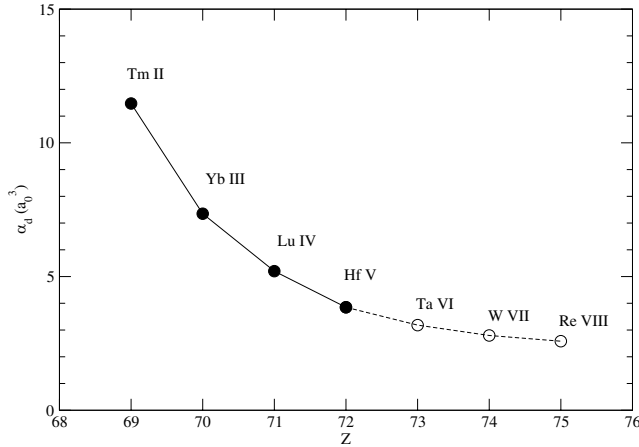

Figure 1. Static dipole polarizability, α_d, in a_0^3 versus the atomic number, Z, along the erbium isoelectronic sequence. Filled circle: values tabulated by Fraga et al. (1976). Open circle: extrapolated values.

computes the atomic structure in a Breit–Pauli relativistic framework. Single-electron orbitals, $P_{nl}(r)$, are constructed by diagonalizing the non-relativistic Hamiltonian within a statistical Thomas–Fermi–Dirac model potential $V(\lambda_{nl})$ (Eissner & Nussbaumer 1969). The λ_{nl} scaling parameters are optimized variationally by minimizing a weighted sum of the *LS* term energies. *LS* terms are represented by CI wavefunctions of the type

$$\Psi = \sum_i C_i \Phi_i.$$

Relativistic fine-structure levels and transition rates are obtained by diagonalizing the Breit–Pauli Hamiltonian in intermediate cou-

pling. The one- and two-body fine-structure and non-fine-structure operators have been fully implemented to the order $\alpha^2 Z^4$ where α is the fine-structure constant and Z the atomic number.

Semi-empirical corrections take the form of term energy corrections (TEC). By considering the relativistic wavefunctions, Ψ_i^r, in a perturbation expansion of the non-relativistic wavefunctions, Ψ_i^{nr},

$$\Psi_i^r = \Psi_i^{nr} + \sum_{j\neq i} \Psi_j^{nr} \frac{\left\langle \Psi_j^{nr} \left| H_{1b} + \dot{H}_{2b} \right| \Psi_i^{nr} \right\rangle}{E_i^{nr} - E_j^{nr}},$$

where H_{1b} and H_{2b} are, respectively, the one-body and two-body parts of both fine-structure and non-fine-structure Hamiltonians. A modified non-relativistic Hamiltonian is constructed with improved estimates of the differences $E_i^{nr} - E_j^{nr}$ so as to adjust the centres of gravity of the spectroscopic terms to the available experimental values.

In this study, two calculations have been carried out in Tc II. In calculation AS1, the same CI expansion as in the HFR calculations has been considered. A similar polarization potential has been included with the corresponding correction to the electric dipole transition operator. The difference with the HFR + CP treatment of the polarization effects is that in AUTOSTRUCTURE, both dielectronic and penetration terms are neglected. We used the same ionic core polarization parameters as in our above-mentioned HFR + CP1 model. The scaling parameters have been optimized by minimizing the sum of all the 1536 *LS* term energies. The optimized values are the following: $\lambda_{1s} = 1.4155$; $\lambda_{2s} = 1.1329$; $\lambda_{2p} = 1.0823$; $\lambda_{3s} = 1.0481$; $\lambda_{3p} = 1.0322$; $\lambda_{3d} = 1.0148$; $\lambda_{4s} = 1.0275$; $\lambda_{4p} = 1.0302$; $\lambda_{4d} = 1.0458$; $\lambda_{5s} = 1.0705$; $\lambda_{5p} = 1.0536$; $\lambda_{5d} = 1.0403$; $\lambda_{6s} = 1.0356$; $\lambda_{6p} = 1.0323$; $\lambda_{7s} = 1.0373$; $\lambda_{7p} = 1.0346$.

Calculation AS2 corresponds to AS1 in which TEC have been applied to the ground term $4d^5(^6S)5s$ a^7S, the first excited even terms $4d^5(^6S)5s$ a^5S, $4d^6$ a^5D and odd terms $4d^5(^6S)5p$ $z^{7,5}P^o$ compiled by

Table 3. Fitted parameter values in Tc II, Mn II, Re II and Mo I.

Configuration	Parameter[a]	Fitted value (cm^{-1})	Ratio[b]
Tc II			
$4d^5 5s$	E_{av}	$40\,038 \pm 7$	
	$G^2(4d,5s)$	$11\,981 \pm 11$	0.82
$4d^6$	E_{av}	$25\,004 \pm 4$	
	ζ_{4d}	712 ± 5	0.92
$4d^5 5p$	E_{av}	$76\,293 \pm 65$	
	ζ_{4d}	1209 ± 117	1.41
	ζ_{5p}	1193 ± 24	1.26
	$G^1(4d,5p)$	5480 ± 27	0.70
	$G^3(4d,5p)$	4362 ± 21	0.70
Mn II			
$3d^5 4s$	E_{av}	$46\,445 \pm 2$	
	$G^2(3d,4s)$	8702 ± 3	0.82
$3d^6$	E_{av}	$38\,667 \pm 1$	
	ζ_{3d}	262 ± 1	0.93
$3d^5 4p$	E_{av}	$83\,621 \pm 5$	
	ζ_{3d}	598 ± 25	1.87
	ζ_{4p}	364 ± 3	1.25
	$G^1(3d,4p)$	4744 ± 2	0.78
	$G^3(3d,4p)$	3835 ± 2	0.78
Re II			
$5d^5 6s$	E_{av}	$39\,646 \pm 256$	
	ζ_{5d}	2648 ± 168	0.91
	$G^2(5d,6s)$	$16\,934 \pm 284$	0.83
$5d^4 6s^2$	E_{av}	$48\,666 \pm 720$	
	ζ_{5d}	2850 ± 180	0.91
$5d^6$	E_{av}	$41\,229 \pm 350$	
	ζ_{5d}	2501 ± 158	0.91
$5d^5 6p$	E_{av}	$88\,994 \pm 2024$	
	ζ_{5d}	4357 ± 507	1.47
	ζ_{6p}	4690 ± 233	1.23
	$G^1(5d,6p)$	8040 ± 2084	0.79
	$G^3(5d,6p)$	6142 ± 1592	0.79
Mo I			
$4d^5 5s$	E_{av}	$32\,108 \pm 0$	
	$G^2(4d,5s)$	$10\,923 \pm 0$	0.79
$4d^5 5p$	E_{av}	$56\,391 \pm 121$	
	ζ_{4d}	1196 ± 165	2.00
	ζ_{5p}	490 ± 41	1.21
	$G^1(4d,5p)$	3467 ± 42	0.56
	$G^3(4d,5p)$	2513 ± 31	0.56

[a]Only the parameters that have been fitted are given. The others were kept at 80 per cent of their HFR values. [b]Ratio = fitted/*ab initio*.

Moore (1958). In this last calculation, the agreement between the length and the velocity gauges was ∼20 per cent for the lines with

$$\log gf \geqslant -1.$$

Our computer limitations have prevented any attempts to either extend further the CI expansions and/or to take into account the two-body relativistic corrections.

3.4 Partition functions in Tc I, Tc II and Tc III

The calculation of ionization equilibrium in stellar atmospheres using Saha equation requires the evaluation of the partition functions for Tc I, Tc II and Tc III. In order to estimate the detrimental effect of missing experimental levels on the partition functions in Tc I and Tc II, two calculations were performed, the first one using only the available experimental levels and the second one based on the experimental levels completed with calculated values.
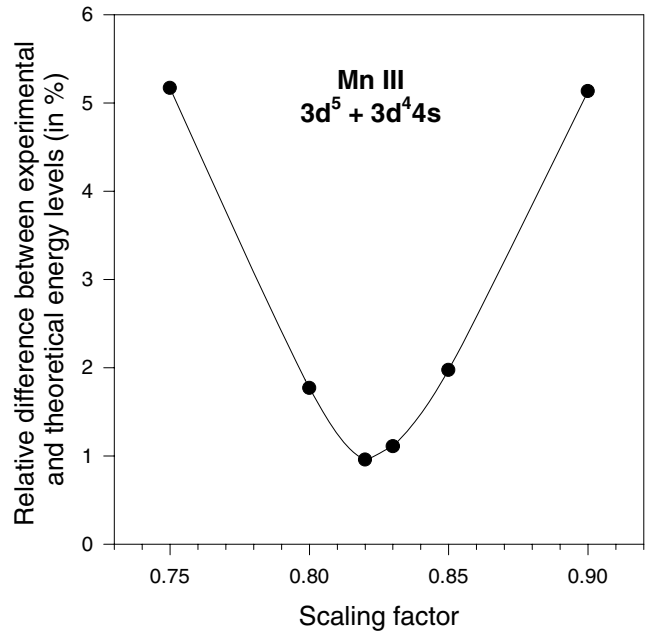
Figure 2. Relative difference between experimental and theoretical energy levels in the $3d^5$ and $3d^4 4s$ configurations of Mn III using different scaling factors for the Slater integrals.

In the case of Tc I, we used the experimental energies given by Palmeri & Wyart (1999) and the calculated values obtained in the semi-empirical HFR model developed by Palmeri et al. (2005a) including the 4216 levels belonging to the $4d^6 ns$, $4d^5 5s^2$, $4d^5 5sns$, $4d^7$, $4d^6 5d$, $4d^5 5s5d$, $4d^4 5s^2 5d$, $4d^5 5p^2$, $4d^6 np$, $4d^5 5snp$ and $4d^4 5s^2 5p$ ($n = 5$–7) configurations.

For Tc II, only 13 experimental levels are reported in the NIST compilation (Moore 1971). These values were completed by the semi-empirical HFR calculations performed in the present work and described in Section 3.2.

In the case of Tc III, for which no experimental level values are available in the literature, the partition functions could only be estimated using theoretically predicted energies. These were obtained using the HFR code of Cowan (1981) including the $4d^5$, $4d^4 5s$ and $4d^5 5p$ configurations, which corresponds to 280 levels between 0 and $172\,000$ cm^{-1}. It was verified that other configurations, such as $4d^3 5s^2$ for example, lie too high in energy to contribute significantly to the partition functions. All the Slater integrals (F^k, G^k and R^k) corresponding to $4d^5$, $4d^4 5s$ and $4d^4 5p$ were scaled down by a factor of 0.82, which was found to be the best value to reproduce all the experimental energy levels listed in the NIST compilation for the $3d^5$ and $3d^4 4s$ configurations in the homologous ion along the 3d period, that is, Mn III. This is illustrated in Fig. 2 showing the influence of the scaling factor on the difference between calculated and experimental energies. Moreover, in order to obtain a more realistic representation of Tc III, the average energies, E_{av}, were adjusted to reproduce the lowest level of the two excited configurations, that is, $4d^4 5s$ and $4d^4 5p$. These values were obtained by interpolation along the 4d period (from Y III to Cd III) and by analogy with the behaviour observed along the 3d period (from Sc III to Zn III) as illustrated in Fig. 3. This procedure allowed us to predict the lowest levels of each configuration in Tc III as follows: $4d^4 5s\ {}^6D_{1/2} = 44\,000$ cm^{-1} and $4d^4 5p\ {}^6F_{1/2} = 89\,000$ cm^{-1}.

The partition functions calculated in the present work are given in Table 4 for temperatures from 3000 to $14\,000$ K while the influence
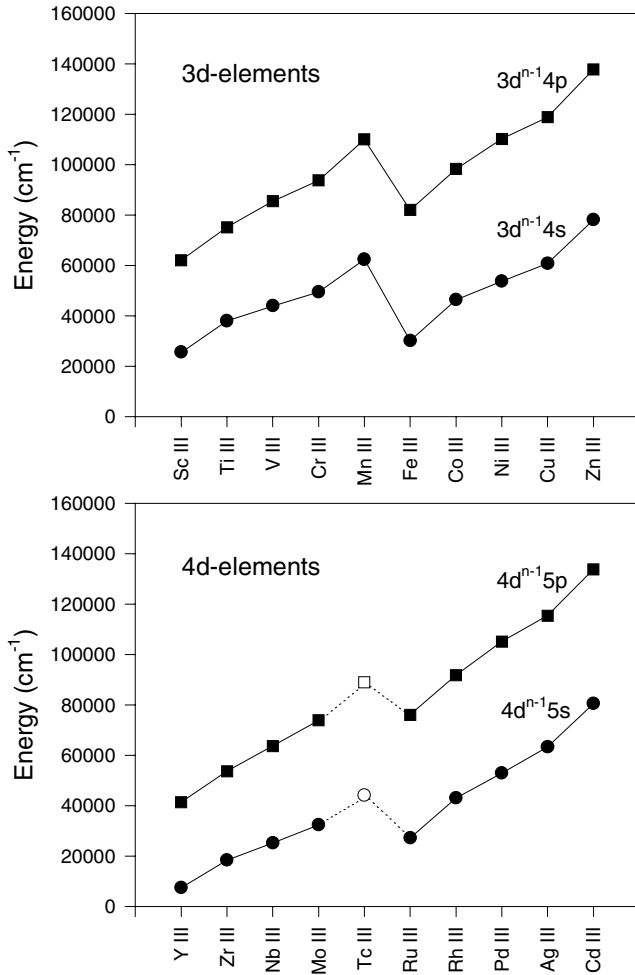
Figure 3. Comparison between the behaviour of the lowest energy level of the $3d^{n-1}4s$ and $3d^{n-1}4p$ configurations along the 3d period and the $4d^{n-1}5s$ and $4d^{n-1}5p$ configurations along the 4d period ($n = 1$–10). Filled symbols represent experimental values while open symbols (for Tc III) represent interpolated values.

of the missing experimental levels for Tc I and Tc II is illustrated in Fig. 4.

4 DISCUSSION OF THE RESULTS

A comparison between the available measured and theoretical radiative lifetimes are given in Table 1 for the $z^{5,7}P^o$ levels in Mn II, Tc II, Re II and Mo I. In Mn II, the beam-laser measurements and the CA calculations of Pinnington et al. (1992) are in between our CP1 and CP2 values. The CP2 lifetimes are definitely too long in Re II and Mo I. In these two species, the CP1 core-polarization model reproduces reasonably well our laser LIF measurements and those of Kwiatkowski et al. (1981) and Schnehage et al. (1983). In Tc II, our CA calculations support also the CP1 lifetimes.

In Table 2, a comparison between our calculated oscillator strengths are presented for the transitions depopulating the $4d^5(^6S)5p$ $z^{5,7}P^o$ levels in Tc II. An excellent agreement is found between the CP1 and CA data sets for the transitions $4d^5(^6S)5s$ a^7S–$4d^5(^6S)5p$ z^7P^o. With regard to the transitions $4d^5(^6S)5s$ a^5S–$4d^5(^6S)5p$ z^5P^o, the agreement is somewhat deteriorated due to stronger mixing effects in the quintet system which cause the CA

Table 4. Partition functions in Tc I, Tc II and Tc III.

| T (K) | Tc I | | Tc II | | Tc III |
	Exp. levels only[a]	Exp. + calc. levels[b]	Exp. levels only[c]	Exp. + calc. levels[d]	Calc. levels[e]
3000	12.6497	12.6499	10.5463	10.5666	6.0033
3500	14.4762	14.4771	11.6802	11.7507	6.0134
4000	16.3781	16.3817	12.7762	12.9582	6.0387
4500	18.4155	18.4267	13.8155	14.2002	6.0892
5000	20.6459	20.6750	14.7916	15.4981	6.1756
5500	23.1166	23.1820	15.7038	16.8744	6.3079
6000	25.8634	25.9956	16.5549	18.3497	6.4949
6500	28.9122	29.1574	17.3492	19.9407	6.7440
7000	32.2805	32.7052	18.0913	21.6602	7.0605
7500	35.9792	36.6755	18.7864	23.5174	7.4482
8000	40.0147	41.1050	19.4391	25.5184	7.9097
8500	44.3893	46.0324	20.0540	27.6673	8.4459
9000	49.1028	51.4992	20.6354	29.9662	9.0569
9500	54.1523	57.5495	21.1870	32.4164	9.7423
10 000	59.5331	64.2308	21.7122	35.0183	10.5006
10 500	65.2386	71.5931	22.2142	37.7718	11.3301
11 000	71.2609	79.6890	22.6956	40.6770	12.2290
11 500	77.5906	88.5722	23.1588	43.7341	13.1950
12 000	84.2173	98.2978	23.6059	46.9435	14.2259
12 500	91.1295	108.9208	24.0387	50.3061	15.3194
13 000	98.3151	120.4956	24.4588	53.8234	16.4734
13 500	105.7611	133.0756	24.8676	57.4973	17.6856
14 000	113.4542	146.7121	25.2663	61.3304	18.9541

[a]Calculated using the experimental energy levels given by Palmeri & Wyart (1999). [b]Calculated using the experimental energy levels given by Palmeri & Wyart (1999) completed with those obtained by the semi-empirical HFR model of Palmeri et al. (2005a). [c]Calculated using the experimental energy levels compiled at NIST (Moore 1971). [d]Calculated using the experimental energy levels compiled at NIST (Moore 1971) completed with those obtained by the semi-empirical HFR model of the present work. [e]Calculated using the HFR energy levels predicted in the present work (see text).

approach to be less relevant. The comparison between AS1 and AS2 illustrates the sensitivity to TEC, especially in the case of the intercombination lines. Our best AUTOSTRUCTURE calculation (AS2) supports the HFR + CP1 model.

In conclusion, we recommend the present HFR + CP1 oscillator strengths in Tc II.

5 A SEARCH FOR TC II ABSORPTION LINES IN STELLAR SPECTRA

The quest for Tc II in stellar atmospheres may seem hopeless, because technetium is known to be synthesized in the interiors of AGB stars: with their surface effective temperatures below 3600 K, AGB stellar atmospheres should contain mostly *neutral* technetium. To fix the ideas, neutral technetium represents 80 per cent of Tc in an AGB atmosphere characterized by an effective temperature of 3400 K.

In fact, the only searches for Tc II lines in stellar spectra date back to Little-Marenin & Little (1987) and Boyarchuk & Snow (1978). The first used the *IUE* satellite and the second the *Copernicus* satellite to look for Tc II λ254.234 nm, 261.000 nm and 264.702 nm in the atmospheres of three barium stars (McClure 1984) and in the A stars Sirius and Vega, respectively, all with negative results. For barium stars, this non-detection confirms the extrinsic-pollution scenario: barium stars owe their chemical peculiarity to mass transfer across a binary system. ^{99}Tc was synthesized, as well as other s-process
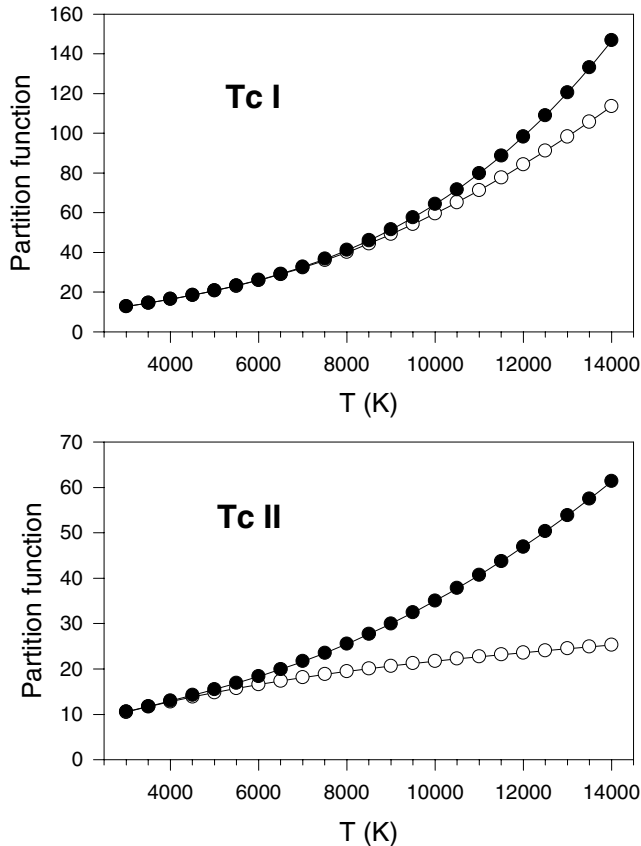
Figure 4. The influence of the missing experimental levels on the calculation of partition functions in Tc I and Tc II. The open circles correspond to the calculation performed with available experimental data only while the filled circles correspond to the calculation performed using available experimental data completed with calculated energies.

elements, a long time ago in an AGB star and transferred to its companion which thus turned into a barium star. With a half-life of only 2.1×10^5 yr, ^{99}Tc had time to decay and is not observed any longer in the polluted barium star atmosphere, unlike the other (stable) s-process elements.

Nevertheless, the search for Tc II lines holds hope in at least two categories of warm peculiar stars:

(i) low-metallicity AGB stars, which follow evolutionary tracks that are bluer and warmer than their solar-metallicity counterpart, so that they may venture in regions of the Hertzsprung–Russel diagram warm enough for technetium to appear in the form of Tc II;

(ii) some Ap stars, where nucleosynthesis processes involving particles accelerated by magnetic fields could account for (some of) the chemical peculiarities, and in particular for the unstable elements, as claimed by Cowley et al. (2004) and Gopka et al. (2004). Much earlier, Davis (1973) already suspected that Tc II lines might be present in the spectra of some Ap stars.

A few stars belonging to the above categories have therefore been scrutinized for the presence of the most intense Tc II lines accessible to ground-based high-resolution spectrographs, hence with $\lambda >$ 330 nm.

5.1 High-luminosity CH stars

The low-metallicity ([Fe/H] $= -3.5$), s-process-rich star CS 30322$-$23 has been studied by Masseron et al. (2006). Its high-

luminosity and low gravity (log $g = -0.3$) clearly locates it on the thermally pulsing part of the AGB, where s-process elements, including Tc, are believed to be produced and dredged up to the stellar surface.

Due to its low metallicity, this star is rather warm ($T_{eff} = 4100$ K) for its category. It is thus an ideal candidate to look for possible lines of ionized Tc, since more than 98 per cent of Tc atoms should be ionized. A tailored model atmosphere belonging to the OSMARCS family (Gustafsson, Edvardsson & Eriksson 2003) has been computed and allowed us to fit the λ 389.2129 and 397.5017 nm Tc II lines through spectral synthesis.

Unfortunately, only upper limits could be derived: $\varepsilon(\text{Tc})/\varepsilon(\text{Zr}) \leqslant$ 0.2, where $\varepsilon(\text{X})$ denotes the abundance of element X. Parametrized s-process calculations in low-metallicity AGB stars (Goriely & Mowlavi 2000) predict $\varepsilon(\text{Tc})/\varepsilon(\text{Zr}) \sim 0.001$. Hence our upper limit mentioned above is not constraining.

Neither were Tc II lines detected in another evolved CH star, V Ari, nor in the spectra of several late-type stars available on the UVES Paranal Observatory Project data base (Bagnulo et al. 2003).

5.2 Chemically peculiar stars

Przybylski star (HD 101065) is a very peculiar rapidly oscillating Ap star (roAp hereafter), its spectrum being characterized by the extreme weakness of iron lines combined to the extreme strength of lanthanide (rare earth) lines. Even more surprising, it has recently been claimed that, on top of these large enhancements in the lanthanides (by 3–4 dex; Cowley et al. 2000), Przybylski star could as well be enriched in many actinides. Several authors even reported the possible detection of technetium (Cowley et al. 2004; Bidelman 2005). In particular, Cowley et al. (2004) observed features at λ (nm) $=$ 321.206 (log $gf = 0.10$), 329.883, 389.205 (log $gf =$ -1.14) and 397.502 (log $gf = -1.60$), close to Tc II lines, but nothing at 319.520 (log $gf = -0.10$) nor at 323.702 (log $gf = 0.24$). We note that the detectability of the Tc II lines listed above does not in any way appear to depend on the log gf value, and moreover that the observed and laboratory line positions sometimes differ by up to 0.008 nm. These two facts obviously cast doubts on their identification as Tc lines, as noted by the authors themselves. They also remark that 'the case for the presence of Tc I seems better than that for Tc II', which is curious for such a warm star ($T_{eff} = 6600$ K), where Saha equation predicts that there would be 99 per cent of Tc II.

A UVES spectrum of Przybylski star reveals that the two most prominent Tc II lines in the near-UV region are unfortunately located in a crowded region of the spectrum, where they would be severely blended (Tc II λ 389.2129 nm by Nd II λ 389.206 nm and Tc II λ 397.5017 nm by Ce II λ 397.507 nm). Hence, a claim for Tc II detection cannot be made safely just on the basis of wavelength coincidence in Przybylski star but would require an adequate spectrum synthesis. Clear evidence for Tc I could not be found either.

The extreme abundance peculiarities of Przybylski star atmosphere have been traditionally explained by radiative diffusion, which is made very efficient thanks to the stabilization of the atmosphere by a strong magnetic field. Any reliable abundance determination in this star must thus await stratified model atmospheres (as well as better atomic data, especially for doubly ionized species).

Apart from Przybylski star, several other high-resolution spectra of chemically peculiar stars are available in the UVES archives. In particular, the UVES Paranal Observatory Project data base (Bagnulo et al. 2003) contains seven A-type stars with strong Sr and/or Eu lines. Their spectra were retrieved and brought to zero redshift.
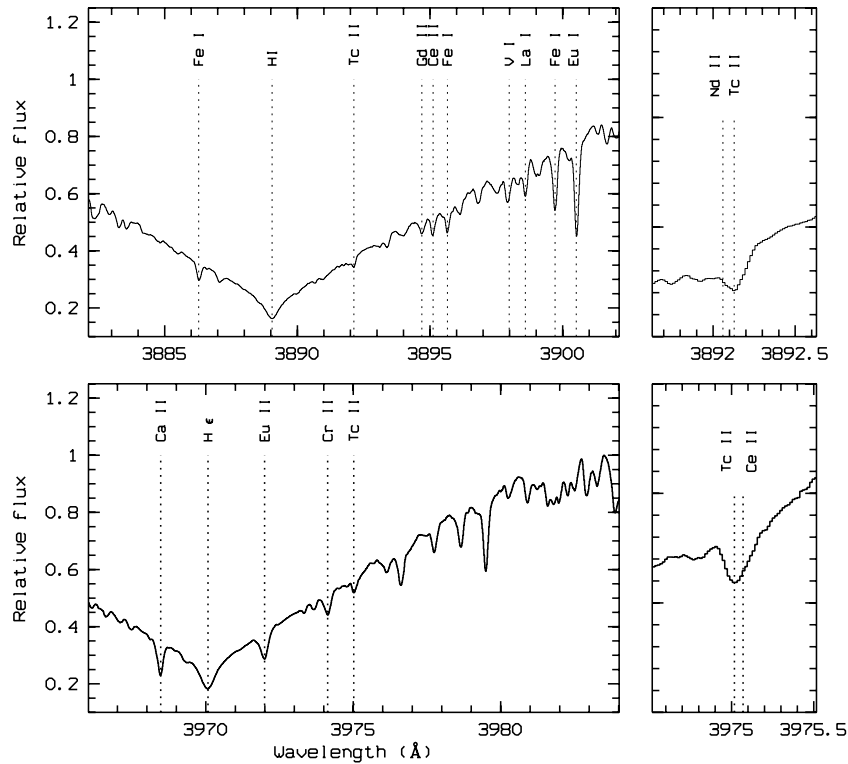
Figure 5. UVES spectra of the Eu–Cr A1 star HD 125248 around the two most prominent near-UV Tc II lines (λ 389.2129 and 397.5017 nm). In each panel the spectrum has been normalized to a nearby continuum point. Several nearby lines are tentatively identified. The right-hand panels zoom on the Tc II lines.

No Tc I lines were observed, which is not surprising given the temperature of these stars: Saha equation predicts the percentages of Tc I, Tc II and Tc III to be 0.3, 99.2 and 0.5 per cent, respectively. As for Tc II, in one instance at least (HD 125248 = CS Vir), wavelength coincidence is observed for the two most prominent Tc II near-UV lines λ 389.2129 and 397.5017 nm. This A1 star of the Eu–Cr peculiarity class (Renson, Gerbaldi & Catalano 1991), with $T_{\mathrm{eff}} = 9375\,\mathrm{K}$ (Hubrig, North & Mathys 2000), has a much cleaner spectrum than Przybylski star, so that line identification through wavelength coincidence is easier.

As shown in Fig. 5, the two near-UV Tc II lines are observed exactly at their rest wavelengths, clearly distinguishable from the location of their respective blending line (Nd II λ 389.206 nm and Ce II λ 397.507 nm).

Quite interestingly, HD 125248 is a well-known spectrum variable with a strong magnetic field, whose effective longitudinal component varies between -2.6 and $2.7\,\mathrm{kG}$ (Bychkov, Bychkova & Madej 2005). The positive extrema of the magnetic field longitudinal component are in phase with the maximum strength of the rare earth lines (Babcock 1951; Mathys 1991). More precisely, Mathys (1992) found inhomogeneities in surface abundances, rare earths and oxygen being more abundant close to the magnetic pole (unlike chromium and silicon). Our tentative Tc II line detection should however await confirmation from spectral synthesis relying on realistic model atmospheres.

ACKNOWLEDGMENTS

REFERENCES

Babcock H. W., 1951, ApJ, 114, 1
Badnell N. R., 1986, J. Phys. B, 19, 3827
Badnell N. R., 1997, J. Phys. B, 30, 1
Bagnulo S., Jehin E., Ledoux C., Cabanac R., Melo C., Gilmozzi R., 2003, The Messenger, 114, 10
Bakhtiyarov A. S., 1988, Afz, 29, 625
Bates D. R., Damgaard A., 1949, Phil. Trans. R. Soc. London, A, 242, 101
Bidelman W. P., 2005, Barnes T. G., III, Bash F. N., eds, ASP Conf. Ser. Vol. 336, Cosmic Abundances as Records of Stellar Evolution and Nucleosynthesis in Honor of David L. Lambert. Astron. Soc. Pac., San Francisco, p. 309
Biémont É., Grevesse N., 1973, ADNDT, 12, 217
Biémont É., Froese Fischer C., Godefroid M. R., Palmeri P., Quinet P., 2000, Phys. Rev. A, 62, 032512
Boyarchuk A. A., Snow T. P., Jr, 1978, ApJ, 219, 515
Bozman W. R., Meggers W. F., Corliss C. H., 1967, JRNBS, 71A, 547
Brown J. A., Smith V. V., Lambert D. L., Dutchover E. J., Hinkle K. H., Johnson H. R., 1990, AJ, 99, 1930
Busso M., Gallino R., Lambert D. L., Raiteri C. M., Smith V. V., 1992, ApJ, 399, 218
Bychkov V. D., Bychkova L. V., Madej J., 2005, A&A, 430, 1143
Catalan M. A., Rico F. R., 1952, An. R. Soc. Esp. Fis. Quim., 48, 334
Cosner K., Truran W., 1981, Ap&SS, 78, 85

Cowan R. D., 1981, The Theory of Atomic Structure and Spectra. University of California Press, Berkeley

Cowley C. R., Ryabchikova T., Kupka F., Bord D. J., Mathys G., Bidelman W. P., 2000, MNRAS, 317, 299

Cowley C. R., Bidelman W. P., Hubrig S., Mathys G., Bord D. J., 2004, A&A, 419, 1087

Davis D. N., 1973, Astrophys. Lett., 14, 217

Eissner W., Nussbaumer H., 1969, J. Phys. B, 2, 1028

Eissner W., Jones M., Nussbaumer H., 1974, Comput. Phys. Commun., 8, 270

Fedchak J., Hartog E. D., Lawler J. E., Palmeri P., Quinet P., Biémont É., 2000, ApJ, 542, 1109

Fraga S., Karwowski J., Saxena K. M. S., 1976, Handbook of Atomic Data. Elsevier Scientific Publishing, Amsterdam

Gopka Vera F., Yushchenko A. V., Shavrina A. V., Mkrtichian D. E., Hatzes A. P., Andrievsky S. M., Chernysheva, Larissa V., 2004, in Zverko J., Ziznovsky J., Adelman S. J., Weiss W. W., eds, IAU Symp. Vol. 224, The A-Star Puzzle. Cambridge Univ. Press, Cambridge, p. 734

Goriely S., Mowlavi N., 2000, A&A, 362, 599

Gustafsson B., Edvardsson B., Eriksson K. et al., 2003, in Hubeny I., Mihalas D., Werner K., eds, ASP Conf. Ser. Vol. 288, Stellar Atmosphere Modeling. Astron. Soc. Pac., San Francisco, p. 331

Hubrig S., North P., Mathys G., 2000, ApJ, 539, 352

Iben I., Jr, Renzini A., 1983, ARA&A, 21, 277

Johnson W. R., Kolb D., Huang K.-N., 1983, ADNDT, 28, 333

Johnson H. R., Ake T. B., Ameen M. M., 1993, ApJ, 402, 667

Jorissen A., Mayor M., 1988, A&A, 198, 187

Jorissen A., Mayor M., 1992, A&A, 260, 115

Jorissen A., Frayer D. T., Johnson H. R., Mayor M., Smith V. V., 1993, A&A, 271, 463

Kwiatkowski M., Micali G., Werner K., Zimmermann P., 1981, Phys. Lett. A, 85, 273

Lindgard A., Nielsen S. E., 1977, ADNDT, 19, 534

Little S. J., Little-Marenin I. R., Hagen-Bauer W., 1987, AJ, 94, 981

Little-Marenin I. R., Little S. J., 1979, AJ, 84, 1374

Little-Marenin I. R., Little S. J., 1987, AJ, 93, 1539

Masseron T., Van Eck S., Famaey B., Goriely S., Plez B., Siess L., Beers T. C., Primas F., Jorissen A., 2006, A&A, 455, 1059

Mathys G., 1991, A&AS, 89, 121

Mathys G., 1992, A&A, 256, L31

McClure R. D., 1984, PASP, 96, 117

Meggers W. F., 1951, JRNBS, 47, 7

Meggers W. F., Scribner B. F., 1950, JRNBS, 45, 476

Merrill P. W., 1952a, ApJ, 116, 21

Merrill P. W., 1952b, Sci, 115, 484

Moore C. E., 1958, Atomic Energy Levels, Vol. III, Natl. Bur. Stand. (US) Circ. 467

Moore C. E., 1971, Atomic Energy Levels Vol. III, NSRDS-NBS 35, US Government Printing Office, Washington DC

O'Malley S. M., Beck D. R., 2003, Phys. Scr., 68, 244

Palmeri P., Wyart J.-F., 1999, J. Quant. Spectrosc. Radiat. Tranfer, 61, 603

Palmeri P., Froese Fischer C., Wyart J.-F., Godefroid M., 2005a, MNRAS, 363, 452

Palmeri P., Quinet P., Biémont E., Xu H. L., Svanberg S., 2005b, MNRAS, 362, 1348

Pinnington E. H., Guo B., Ji Q., Berends R. W., Ansbacher W., Biémont E., 1992, J. Phys., B25, L475

Renson P., Gerbaldi M., Catalano F. A., 1991, A&AS, 89, 429

Schatz G., 1983, A&A, 122, 327

Schnehage S. E., Danzmann K., Künnemeyer R., Koch M., 1983, J. Quant. Spectrosc. Radiat. Tranfer, 29, 507

Shore B. W., Menzel D. H., 1965, ApJS, 12, 187

Smith V. V., Lambert D. L., 1987, AJ, 94, 977

Smith V. V., Lambert D. L., 1988, ApJ, 333, 219

Smith V. V., Lambert D. L., 1990, ApJS, 72, 387

Straniero O., Gallino R., Busso M., Chieffi A., Raiteri C. M., Limongi M., Salaris M., 1995, ApJ, 440, L85

Sugar J., Corliss C., 1985, J. Phys. Chem. Ref. Data, 14, Suppl. 2

Van Eck S., Jorissen A., 1999, A&A, 345, 127

Van Eck S., Jorissen A., 2000, A&A, 360, 196

Wahlgren G. M., Johansson S. G., Litzén U., Gibson N. D., Cooper J. C., Lawler J. E., Leckrone D. S., Engelman R., 1997, ApJ, 475, 380

Whaling W., Brault J. W., 1988, Phys. Scr., 38, 707

White H. E., Eliason A. Y., 1933, Phys. Rev., 44, 753

This paper has been typeset from a MS word document provided by the author.